Supplementary Materials for

Sequence spinning Axially Encoded Metafibers

Jingyu Ma, Yingjun Liu, Chao Gao*, Zhen Xu*

*Corresponding author. Email: zhenxu@zju.edu.cn (Z.X.)

This PDF file includes:

Figs. S1 to S18
Table S1
Legends for movies S1 to S5

Other Supplementary Materials for this manuscript include the following:
Movies S1 to S5

Supplementary Figures

Supplementary Tables

Supplementary Information

Supplementary Figures.

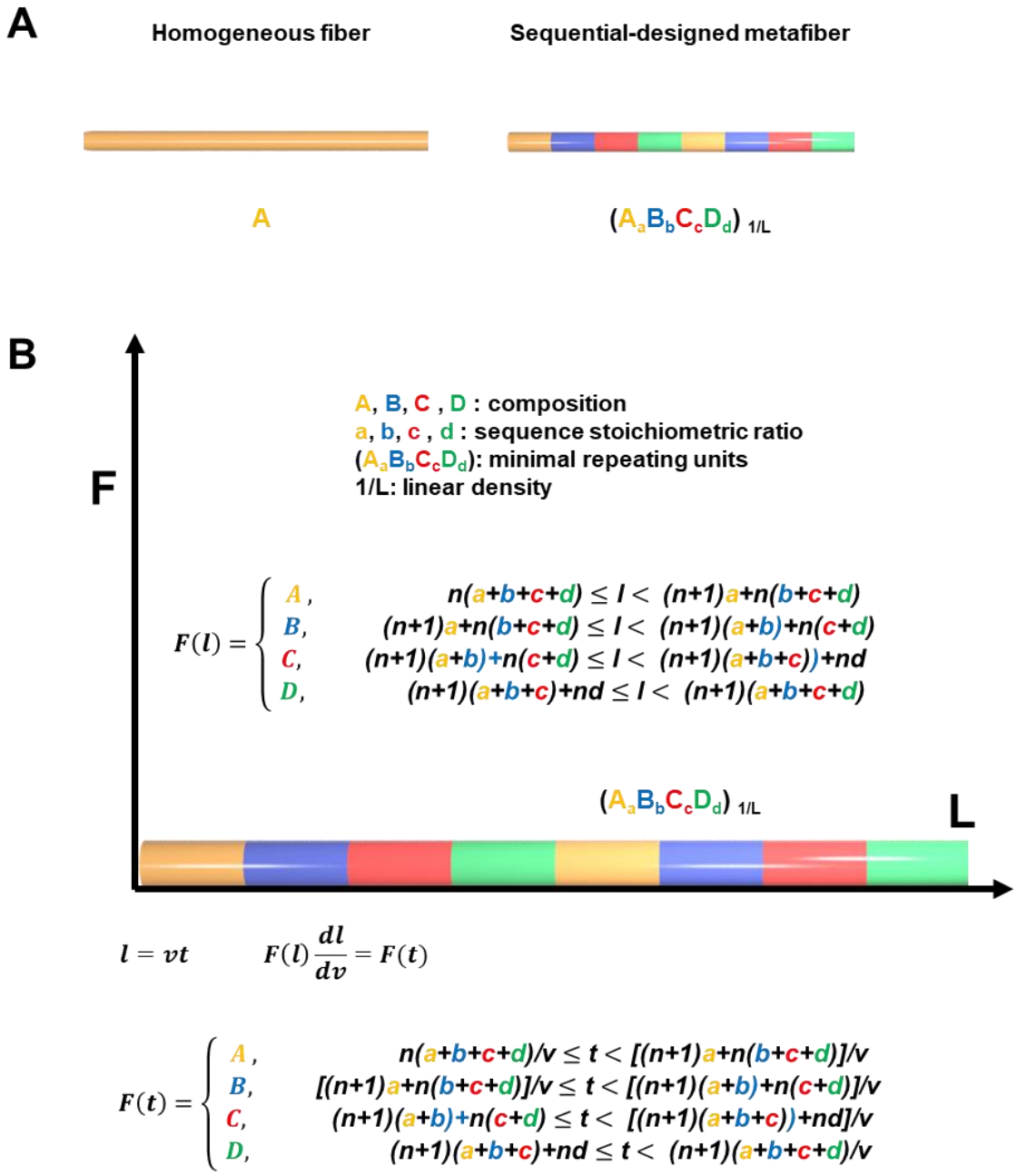

Fig. S1. Mathematical model of axially encoded metafiber. (A) Nomenclature of homogeneous fiber and axially encoded metafiber. (B) Model of sequence spinning axially encoded metafibers.

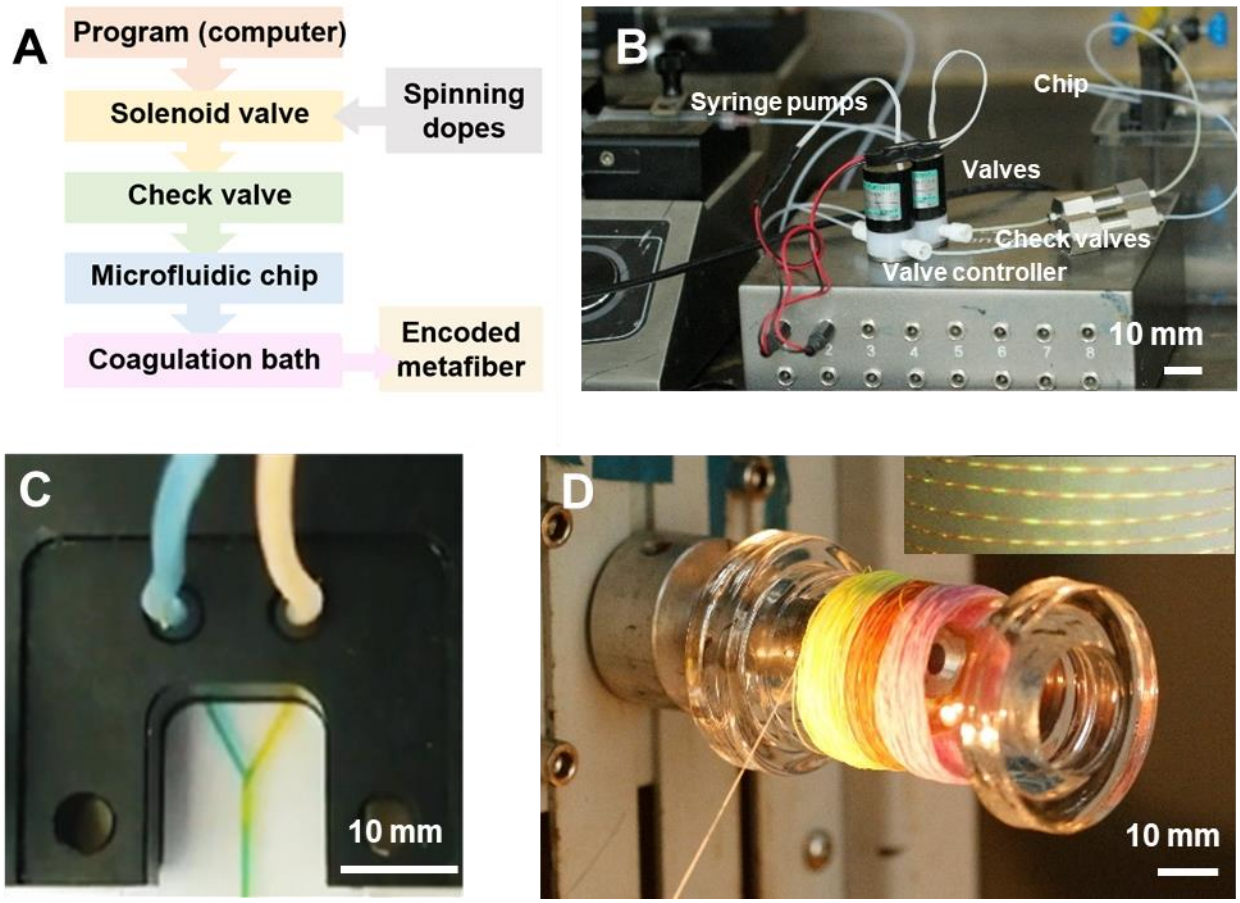

Fig. S2. Sequence spinning process. (A) Flow chart of sequence spinning axially encoded metafibers. (B) MSS system. (C) The designed microchip. (D) The metafiber collector, inset is the luminescent axially encoded metafiber.

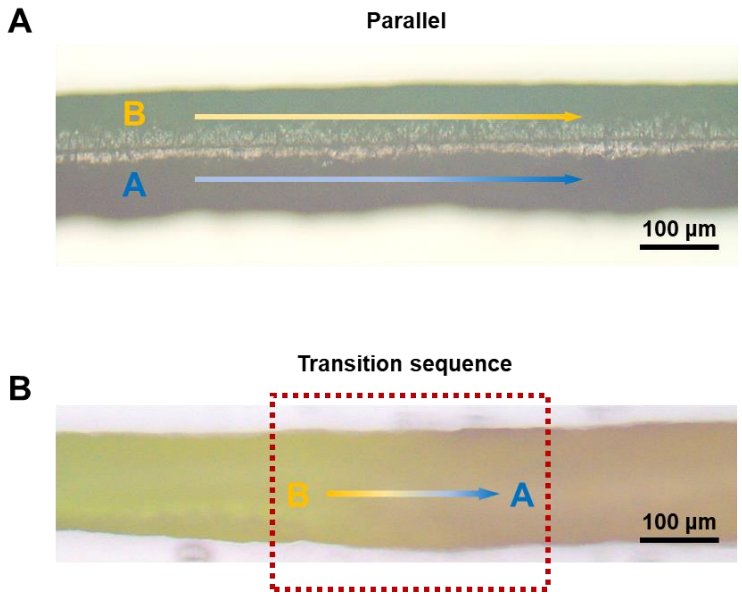

Fig. S3. Images of heterogenous metafibers. (A) A parallel metafiber. (B) A sequence encoded metafiber.

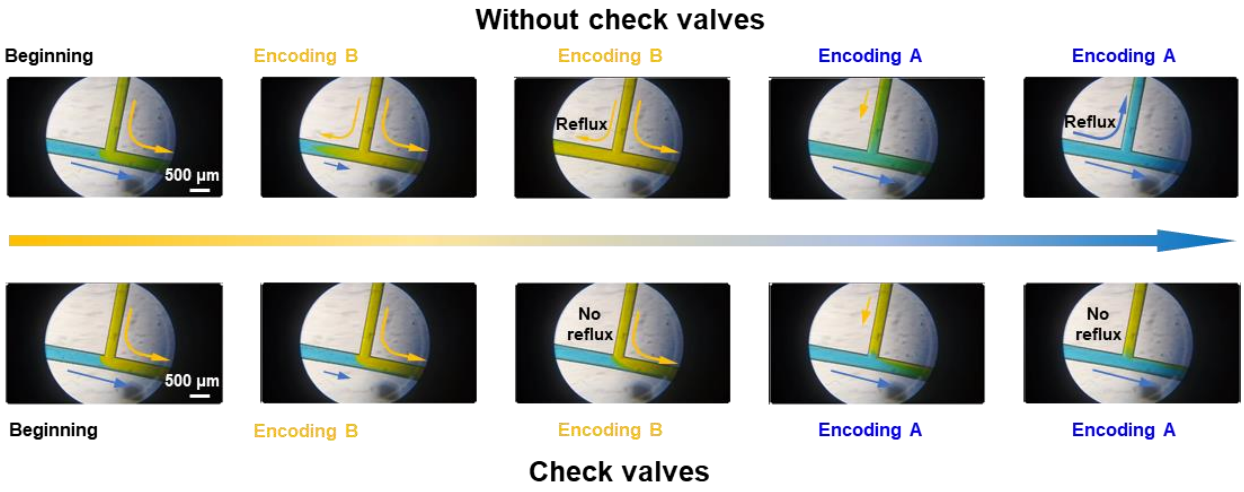

Fig. S4. In-situ observation of the reflux. (A) Images of encoding spinning dopes with/without check valves.

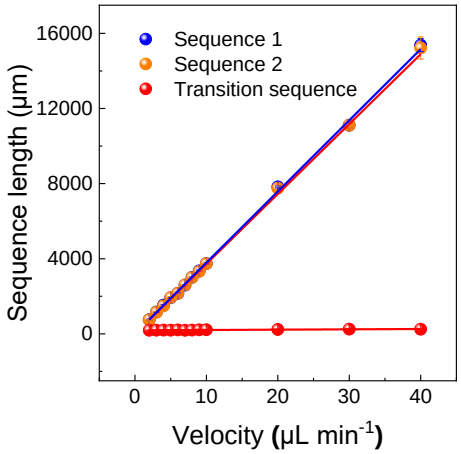

Fig. S5. The relationship between sequence length and spinning velocity. The plot of sequence length as a function of spinning velocity (spinning time: 1s).

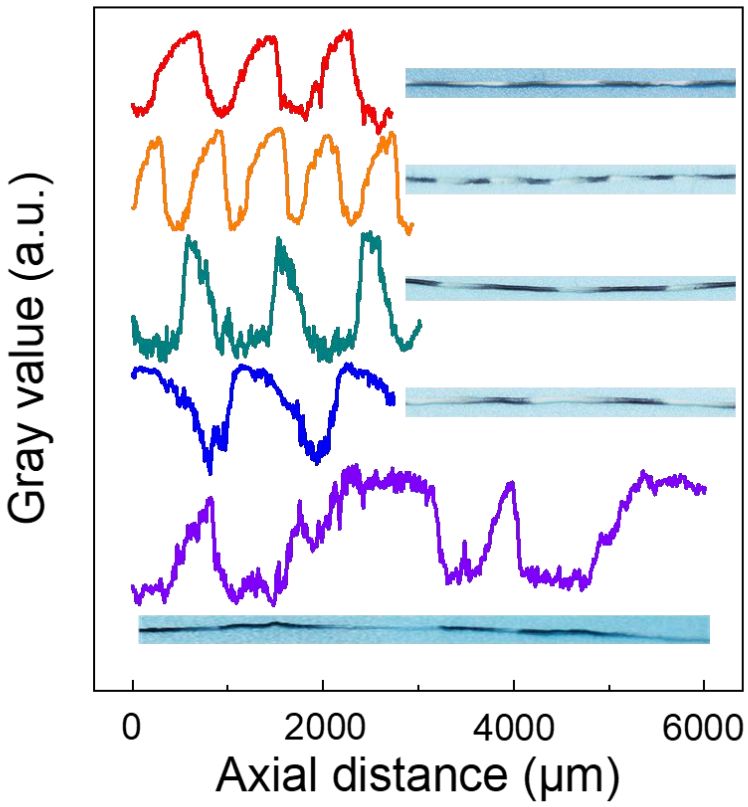

Fig. S6. Information encoding and decoding in metafibers. Images and gray value analysis of encoded metafibers.

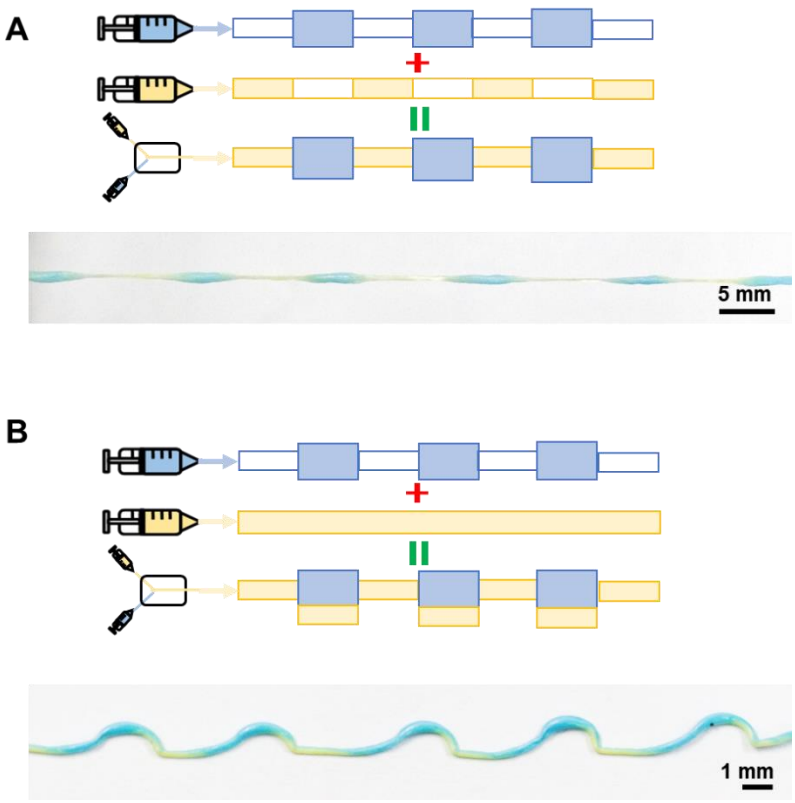

Fig. S7. Multi-morphology metafibers. (A) Schematic and image of the “spindle-shaped” metafiber. (B) Schematic and image of the “sickle-shape” metafiber.

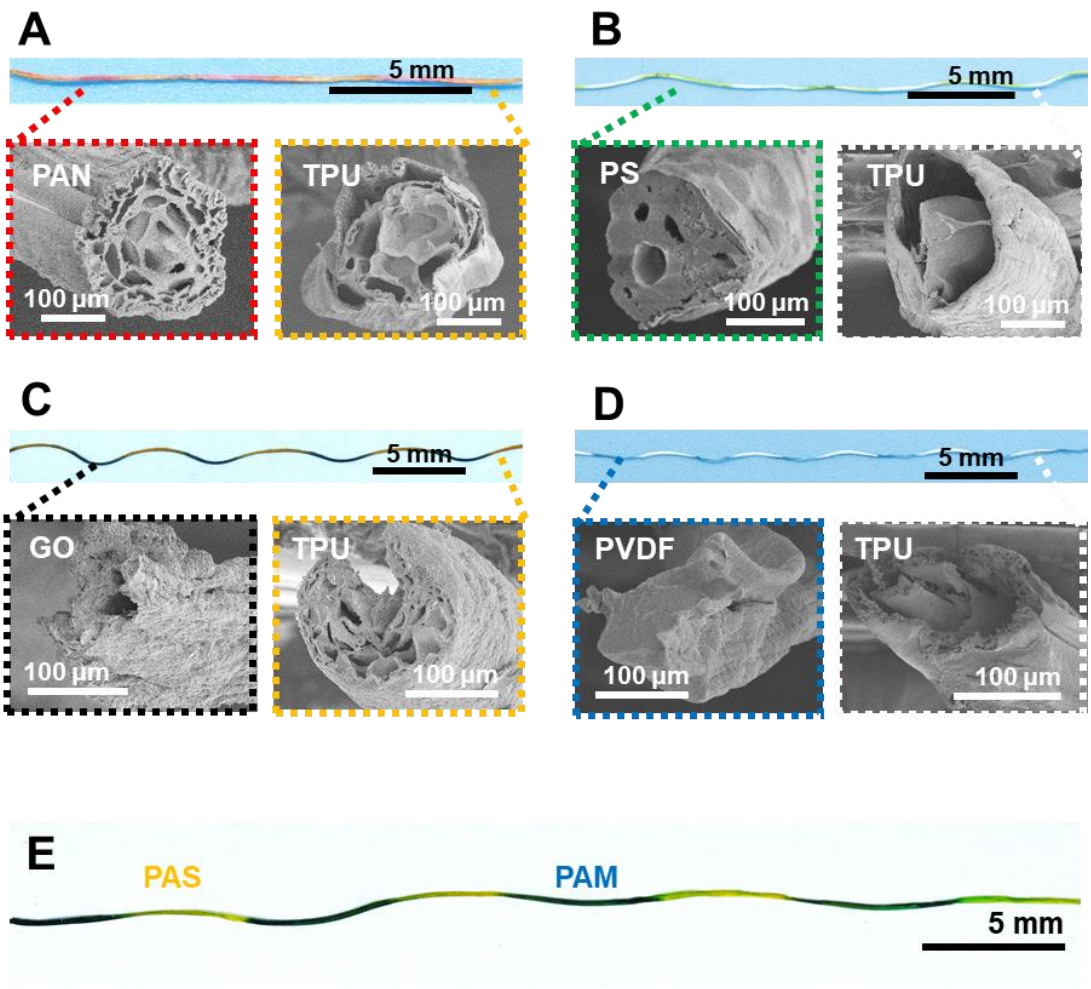

Fig. S8. Multi-material metafibers. (A) A PAN-TPU metafibers. (B) A PS-TPU metafiber. (C) A GO-TPU metafiber. (D) A PVDF-TPU metafiber. (E) A PAS-PAM metafiber.

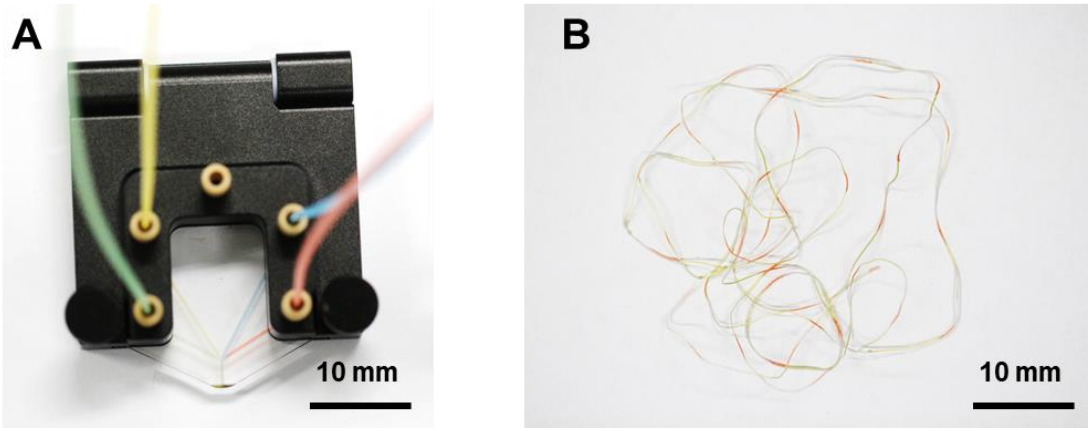

Fig. S9. Multi-material metafibers. (A) The designed 4-channel microchip. (B) A continuous freestanding PAN-PVDF-PS-PMMA metafiber.

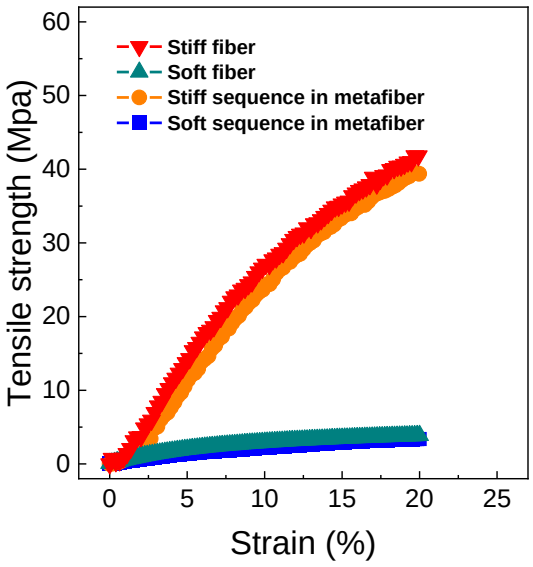

Fig. S10. Varied axial mechanical properties of the mechano-metafiber. Stress-strain curve of the neat fibers and the sequences in mechano-metafiber.

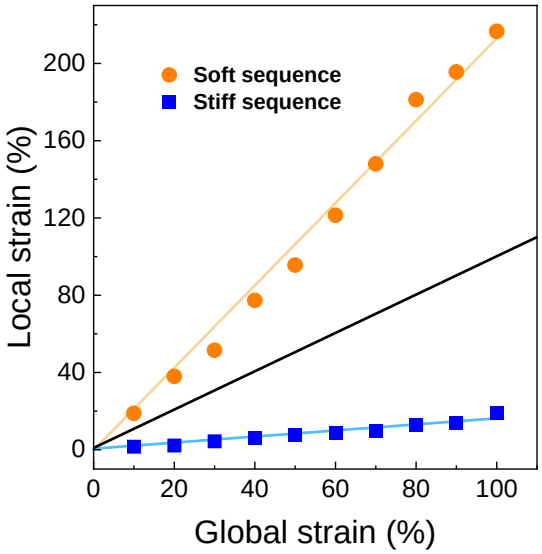

Fig. S11. Localized strain of the mechano-metafiber. Local strain of stiff and soft sequences as a function of the global strain of the whole metafiber.

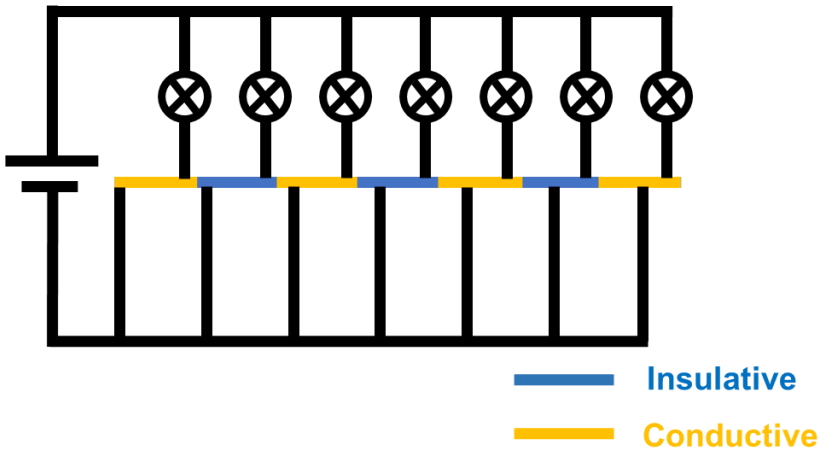

Fig. S12. Schematic of the electro-metafiber connected circuit. The electro-metafiber was connected to a parallel circuit. Each sequence was connected to a LED lamp, respectively.

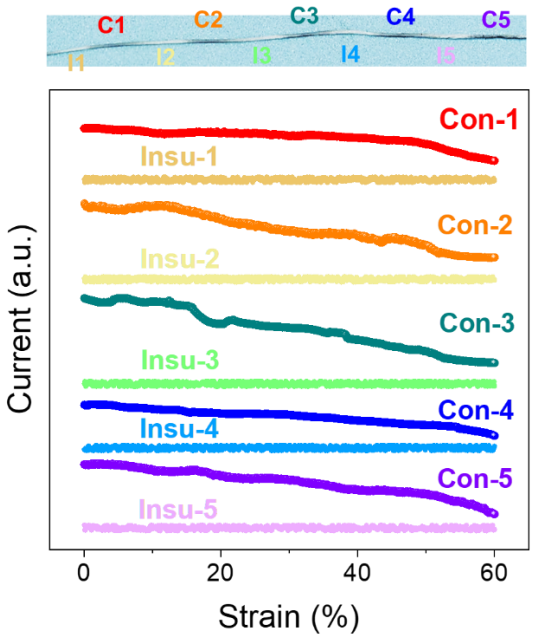

Fig. S13. Localized sensing of the electro-metafiber. Current-strain curves of each sequence.

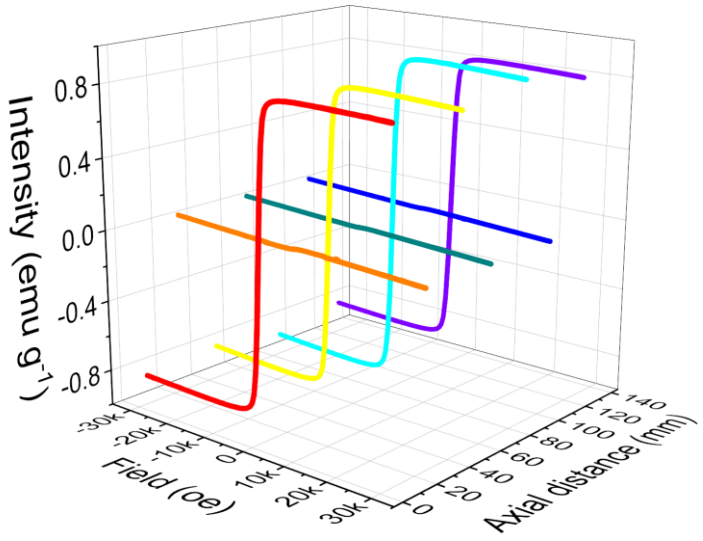

Fig. S14. Varied axial magnetization strength of the magnetic-metafiber. Magnetization curves of each sequence of the magnetic-metafiber from -3T to 3T.

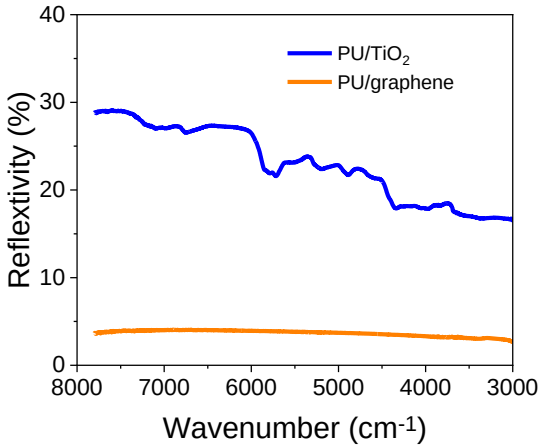

Fig. S15. Infrared reflectivity of the PU/TiO_2 and PU/graphene. IR reflectivity as a function of wavenumber of PU/TiO_2 and PU/graphene.

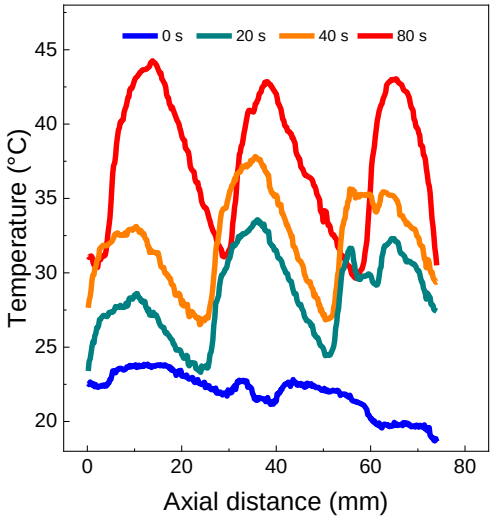

Fig. S16. Localized photothermal properties of the photothermo-metafibers. Temperature as a function of the axial distance of the photothermo-metafiber at different IR exposure time.

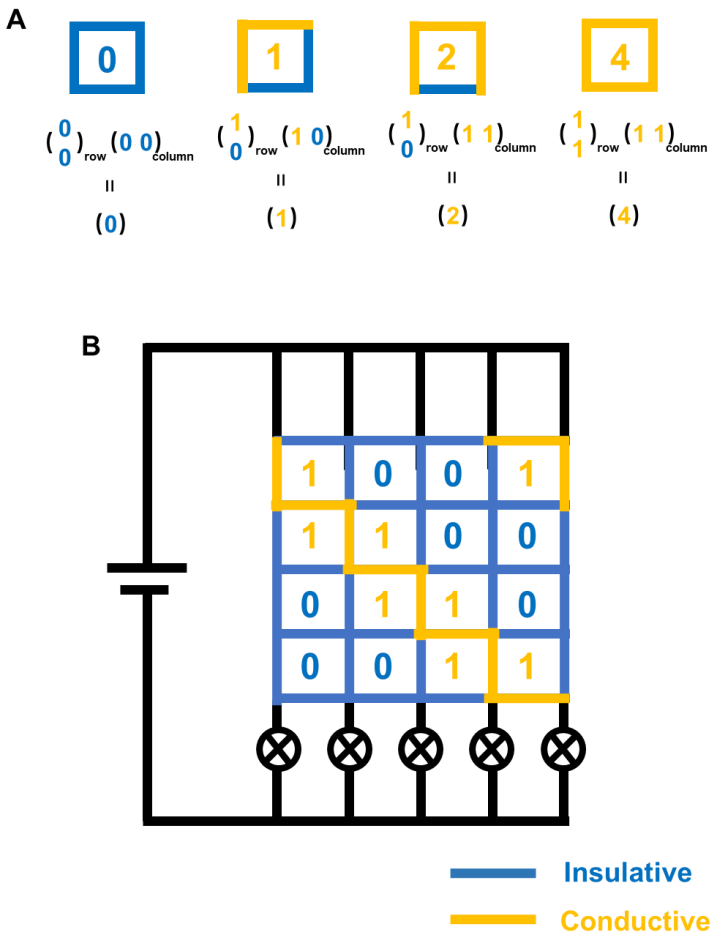

Fig. S17. Matrix operation of the electro-metafibers. (A) Typical representing matrix operation modules. We defined the matrix operation as the sum up of the multiples of adjacent code in a single rectangle. The calculated value demonstrates the number of conductive paths (0, 1, 2, 4) through the rectangle diagons. When the calculated value is 0, the rectangle is insulative; When the value is over 0 (1, 2, 4), the rectangle is conductive through the rectangle diagons. **(**B) Circuit of the woven electro-metafibers.

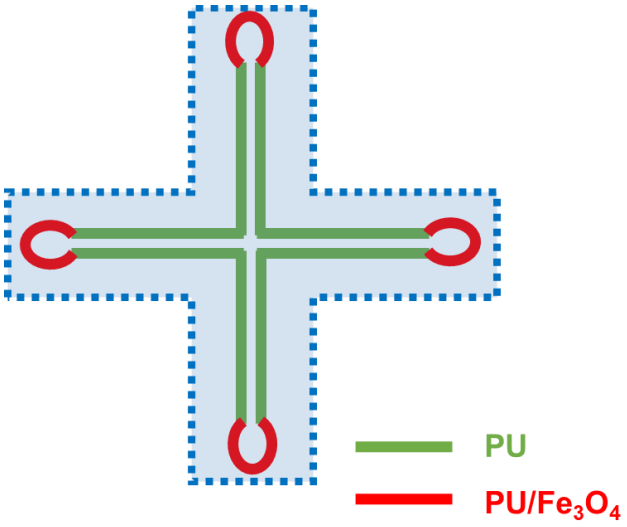

Fig. S18. Magnetic clip of the woven magnetic-metafiber. The PU sequences were woven into the middle area and the ferromagnetic sequences were used as the clip at the edges.

Table S1. List of the designed multi-material metafibers.

Metafibers	Channel A	Channel B	Channel C	Channel D	Solvent	Coagulation bath
PAN-TPU	Polyacrylonitrile (15 wt%)	Polyurethane (15 wt%)			DMF	H_2O
PS-TPU	Polystyrene (15wt%)	Polyurethane (15 wt%)			DMF	H_2O
PVDF-TPU	Polyvinylidene fluoride (15 wt%)	Polyurethane (15 wt%)			DMF	H_2O
PMMA-TPU	Polymethyl methacrylate (15 wt%)	Polyurethane (15 wt%)			DMF	H_2O
PS-PAN	Polyacrylonitrile (15 wt%)	Polystyrene (15wt%)			DMF	H_2O
PAN-PVDF-PMMA	Polyacrylonitrile (15 wt%)	Polyvinylidene fluoride (15 wt%)	Polymethyl methacrylate (15 wt%)		DMF	H_2O
PAN-PMMA-PS-PVDF	Polyacrylonitrile (15 wt%)	Polymethyl methacrylate (15 wt%)	Polystyrene (15wt%)	Polyvinylidene fluoride (15 wt%)	DMF	H_2O
GO-Alg	GO (0.5 wt%)	Alginate (2 wt%)			H_2O	$CaCl_2$/ H_2O
PAS-PAM	Sodium polyacrylate (2 wt %)	Polyacrylamide (2 wt %)			H_2O	$CaCl_2$/ H_2O
CMC-PAM-Alg-PAS	Carboxymethyl cellulose (2 wt%)	Polyacrylamide (2 wt %)	Alginate (2 wt%)	Sodium polyacrylate (2 wt %)	H_2O	$CaCl_2$/ H_2O

Movie S1.
Sequence spinning axially encoded metafibers.

Movie S2.
Sequence spinning process in the microchip.

Movie S3.
Localized strain of a mechano-metafiber under tensile.

Movie S4.
Localized response of a magnetic-metafiber under a magnet.

Movie S5.
The 2D IR movie of a photothermo-metafiber.